



Solubility of corundum in aqueous KOH solutions at 700 °C and 1 GPa

Anke Wohlers*, Craig E. Manning

Department of Earth and Space Sciences, University of California Los Angeles, Los Angeles, California 90095-1567, USA

ARTICLE INFO

Article history:

Received 13 July 2008

Received in revised form 30 January 2009

Accepted 30 January 2009

Editor: J. Fein

Keywords:

Al solubility

Equilibrium constants

Piston cylinder experiments

High *P*

High *T*

ABSTRACT

The solubility of corundum in aqueous KOH solutions was measured at 700 °C and 1 GPa, using a piston-cylinder apparatus and a weight-loss method. Total potassium molality (m_K) ranged from 0.0011 to 3.9. At the lowest m_K , corundum solubility (m_{Al}) was 0.0016 ± 0.0004 molal, which is slightly higher than that in pure H₂O at the same conditions (0.0011 molal). Corundum solubility increased with added KOH to a maximum of $m_{Al} = 2.66$ at the highest m_K . At $m_K \geq 0.03$, m_{Al} increased linearly with m_K , with $dm_{Al}/dm_K = 1$. The results were combined with previous work to evaluate the stability of the neutral ion-pair $KAlO_{2,aq}$ at 700 °C and 1 GPa. We obtained an optimal fit to the experimental data with an equilibrium constant (K) for the reaction $KOH_{aq} = K^+ + OH^-$ of $10^{-1.206}$, which was extrapolated from the data of Ho and Palmer [Ho, P.C. and Palmer, D.A., 1997. Ion association of a dilute aqueous potassium chloride and potassium hydroxide solutions to 600 °C and 300 MPa determined by electrical conductance measurements. *Geochimica et Cosmochimica Acta*, 61, 15, 3027–3040.] using linear isothermal correlations between the logarithms of H₂O density and K . This gave an equilibrium constant for the reaction $KAlO_{2,aq} = K^+ + AlO_2^-$ of $10^{-0.299}$. The results permit assessment of the dominant aqueous species in K–Al–O–H fluids at high pressure and temperature. We find that the dominant Al-bearing species in such fluids is predicted to be the neutral hydrate ($HAIO_{2,aq}$) at $m_K < 0.01$ (pH < 4.8), whereas AlO_2^- predominates to higher m_K and pH, over most geologically realistic conditions. The $KAlO_{2,aq}$ ion pair will only be the most abundant Al-bearing species at very high pH (> 8), which corresponds to KOH molality of > 10 at 700 °C and 1 GPa. Thus, $KAlO_{2,aq}$ is not a major reservoir for dissolved aluminum in low-chloride crustal and mantle aqueous fluids.

© 2009 Elsevier B.V. All rights reserved.

1. Introduction

Aluminum is generally assumed to be immobile during crustal metamorphic and metasomatic processes (e.g., Carmichael, 1969). This is supported by the relatively low solubility of corundum (Al₂O₃) in H₂O at high pressure (*P*) and temperature (*T*) (Becker et al., 1983; Ragnasdottir and Walther, 1985; Walther, 1997; Tropper and Manning, 2007). However, the amphoteric nature of the aqueous Al hydroxides dictates that corundum solubility is enhanced by raising or lowering pH. Hemley and Jones (1964) suggested that Al mobility was promoted by acid leaching by magmatic fluids, and this approach has been widely applied to explain Al-rich veins and segregations in metamorphic rocks (e.g., Yardley, 1977; Kerrick, 1988; Nabelek, 1997; McLelland et al., 2002). High corundum solubility will also be associated with high-pH fluids, as illustrated in the experimental investigations of corundum solubility in KOH solutions reported by Barns et al. (1963), Anderson and Burnham (1967), Pascal and Anderson (1989) and Azaroual et al. (1996). Characterization of Al solubility at high pH is important because model crustal mineral assemblages, such as feldspar + mica +

quartz, in equilibrium with an internally derived H₂O-rich pore fluid, will buffer pH at values more alkaline than neutrality (e.g., Walther and Woodland, 1993).

A key problem that has arisen in the study of Al solubility in alkaline solutions at metamorphic pressures and temperatures is the extent of complexing between alkalis and Al. Experimental investigations of Anderson and Burnham (1967, 1983), Woodland and Walther (1987), Pascal and Anderson (1989), Castet et al. (1992), Diakonov et al. (1996), and Azaroual et al. (1996) argue for alkali–aluminate complexing to explain the high concentration of aluminum in solution. In contrast, Walther and Woodland (1993) presented data on the solubility of the assemblage microcline + muscovite + quartz in H₂O at 0.2 GPa between 400 and 600 °C, and showed that an explanation was possible without including an alkali–aluminate complex, and that the aluminum concentration can be interpreted by the increasing solubility of the aluminate ion with pH. The different interpretations could be due in part to uncertainties in extrapolated equilibrium constants (Anderson, 1995; Azaroual et al., 1996).

The experimental studies described above were limited to low to moderate pressures (≤ 0.6 GPa) and therefore do not give insight into the role of pH and alkalis at high pressure and temperature, where Al mobility can be substantial (e.g., Kerrick, 1988; Ague, 1995; Widmer and Thompson, 2001; Beitter et al., 2008). To address this, we measured corundum solubility in aqueous KOH solutions at 1 GPa at 700 °C. The results are the first experimental measurements of Al

* Corresponding author. Present address: Institute of Mineralogy and Petrography, ETH Zurich, 8092 Zurich, Switzerland. Tel.: +41 44 632 7816.

E-mail address: anke.wohlers@erdw.ethz.ch (A. Wohlers).

Table 1
Experimental results at 700 °C and 1 GPa.

Exp. no	Duration (h)	Type	KOH solution in (mg)	Cor in (mg)	Cor out (mg)	m_k (mol/kg H ₂ O)	m_{Al} (mol/kg H ₂ O)
KOH 2	45.5	b,s	35.314	32.6999	32.6975	0.0011	0.0013(2)
KOH 1	46	b,c	39.271	6.5800	6.5760	0.0011	0.0020(1)
KOH 10	45.5	a,s	34.272	32.9015	32.8965	0.0012	0.0028(2)
KOH 9	48.5	a,s	30.670	33.0540	33.0485	0.0020	0.0036(2)
KOH 7	42.5	b,s	34.994	32.9098	32.8968	0.0079	0.0073(2)
KOH 8	46.5	a,s	30.801	32.6494	32.6239	0.0277	0.0187(2)
KOH 3	48	b,s	35.147	32.6826	32.5616	0.1017	0.0685(2)
KOH 5	44	b,c	34.416	1.2862	0.6941	0.5085	0.3421(2)
KOH 4	46	b,s	34.690	32.6500	31.4653	1.0099	0.7107(2)
KOH 6	46	b,s	36.296	32.9821	28.9439	3.9206	2.6623(3)

Run type: a, diluted 10% W/V KOH solution; b, KOH chip; c, Corundum chip; s, corundum sphere. Parenthetical numbers in solubility entries reflect propagated weighing errors (1 σ).

solubility in aqueous KOH solutions above 0.6 GPa. They provide a foundation for investigations of Al solubility, assessment of the stability of the $KAlO_{2,aq}$ ion pair, and quantifying species abundance in aqueous fluids of the deep crust and upper mantle.

2. Experimental methods

Two types of corundum starting material were used. Most experiments utilized high-purity spheres of synthetic corundum (Tropper and Manning, 2007). The spheres were ~33 mg in weight, ~2.5 mm in diameter, and contained no constituents detectable by electron microprobe analysis other than Al_2O_3 . For two experiments, we used small chips from a synthetic corundum boule (~0.5–1 mm), also pure Al_2O_3 at the limits of detection. Before loading, the chips

were smoothed using sandpaper (Newton and Manning, 2006, 2007, 2008).

The KOH solutions were prepared in two ways. In the first, a reagent-grade KOH chip was dried at 110 °C, weighed, and then added immediately to a precisely determined mass of nanopure H₂O. All such solutions were subsequently reweighed to check mass balance. In the second method, a reagent-grade 10% W/V aqueous KOH solution (Ricca Chemicals) was diluted to the desired concentration using density data from Akerlof and Bender (1941).

For each experiment, a single corundum sphere or chip was loaded into a 1.8 cm long Pt capsule of 3.5 mm diameter and 0.2 mm wall thickness, which had been welded on one side. After addition of aqueous KOH solution, the capsule was sealed by arc welding. Welded seams of each capsule were inspected for holes using a binocular microscope then held at 110 °C for at least 2 h and reweighed to ensure that the capsules did not leak. As in the investigation of Newton and Manning (2008), the corundum crystals proved to be mechanically coherent, which obviated the need for the inner capsules used in some solubility studies in our laboratory (e.g., Antignano and Manning, 2008a,b).

Run conditions were 700 °C and 1 GPa. All experiments were conducted with a 2.54 cm diameter end-loaded piston-cylinder apparatus with sodium chloride pressure media and 1.25 cm diameter graphite heater-sleeves (Manning and Boettcher, 1994). Flattened and folded capsules were placed horizontally in the center of the furnace, packed in NaCl, and covered with a 0.1 mm thick Pt foil to prevent thermocouple puncture. Experiments were pressurized to 0.8 GPa at room temperature and then heated to 700 °C. Heating brought the final pressure to ~1 GPa; only small pressure adjustments were necessary to prevent overshooting. Temperature was maintained to within ± 1 °C using Pt–Pt₉₀Rh₁₀ thermocouples, considered accurate

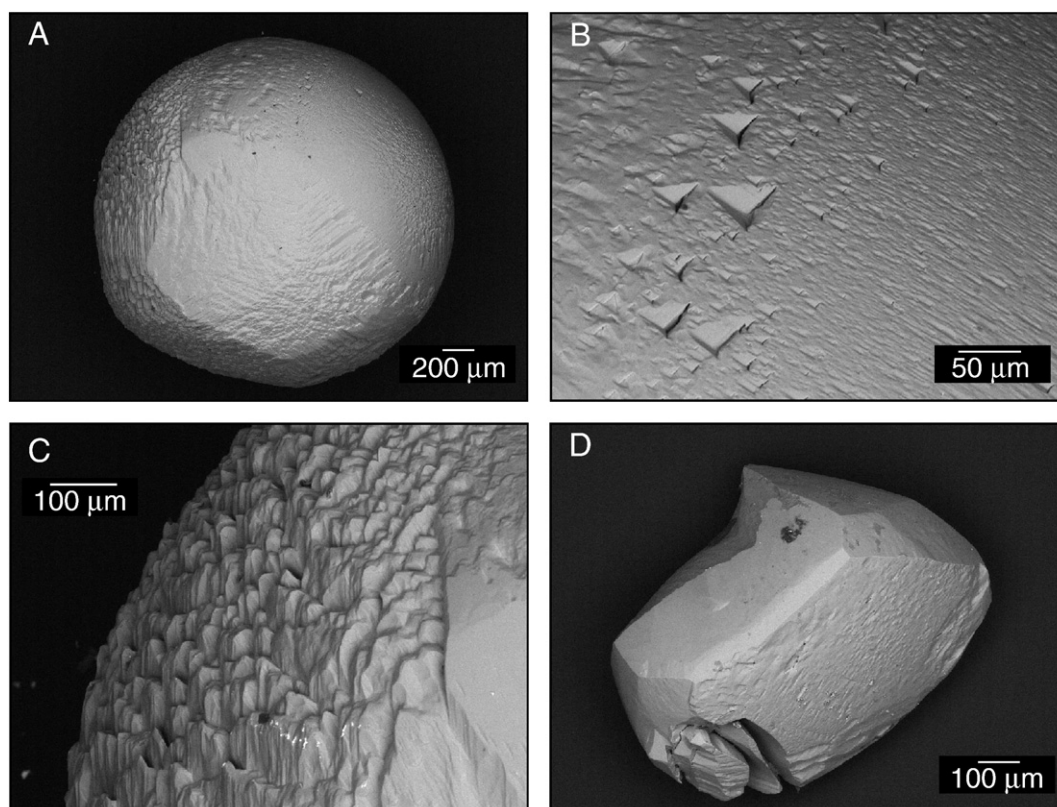


Fig. 1. Backscattered-electron (BSE) photomicrographs of representative corundum textures after experiments. (A) Initially spherical corundum crystal showing etch pits and crude facets that probably developed due to crystallographically controlled dissolution and reprecipitation (KOH 6) (Table 1). (B) Enlargement of sphere shown in (A) illustrating etch pits created by partial dissolution (KOH 6) (Table 1). (C) Irregular corundum terminations suggesting dissolution and reprecipitation. (D) Corundum chip showing smooth, newly grown facets exposed to the solution, and etch-pitted face interpreted to be the base of the crystal, which was in contact with the Pt capsule.

to within ± 3 °C. No correction was made for the effect of pressure on emf. Pressure was measured with a Heise bourdon-tube gauge, and held to ± 0.02 GPa during runs.

Experiments were quenched to <100 °C in <30 s. After quench, the capsule was extracted from the furnace, weighed, pierced with a needle, and then dried for 20 min at 110 °C to check the fluid mass balance. Mass balance was in all cases obtained to within ± 0.33 wt.%. Starting solution weight was used to calculate the reported molalities (Table 1). The dried capsule was carefully opened with a razor blade and the corundum sphere or chip was extracted, cleaned of loosely adhering quench by wiping with a tissue, then rinsed, dried, and weighed. Experimental run products were examined by optical and scanning-electron microscopy. Corundum solubility is reported as Al molality (m_{Al}), determined by crystal weight change using a Mettler UMX2 ultra-microbalance, with a precision of $0.2 \mu\text{g}$ (1σ). Solution weights were determined with a Mettler M3 microbalance ($1\sigma=2 \mu\text{g}$). Reported uncertainties in solubility reflect propagated weighing errors.

3. Results

Results of the experiments on corundum solubility in aqueous KOH solutions at 1 GPa and 700 °C are presented in Table 1 and Figs. 1 and 2. Run durations were ~ 2 days (Table 1). This was assumed adequate for equilibrium for three reasons. First, Becker et al. (1983) studied corundum solubility in H_2O at 670–700 °C and 0.5 GPa, and found no detectable change in solubility in runs of 6–160 h duration. In addition, at 800 °C, 1 GPa, Tropper and Manning (2007) found that equilibration times were <12 h. Finally, corundum dissolution in aqueous KOH solution is expected to have a more rapid dissolution rate than in pure H_2O .

Representative textures are shown in Fig. 1. The surfaces of corundum spheres (Fig. 1A) are decorated with etch pits of varying size (Fig. 1B). Where solubility was high, the spheres showed a tendency to develop crude facets (Fig. 1A), implying a crystal–chemical control on the magnitude of material removed from different portions of the sphere. In some cases, small corundum terminations developed on the sphere surface (Fig. 1C). In experiments using a single corundum chip, the original chips show etch pits on the base of the grain where it sat on the Pt capsule, and strong faceting on other surfaces (Fig. 1D).

A problem commonly encountered in studies of low-solubility minerals such as corundum is the nucleation and growth of new crystals during experiments (e.g., Caciagli and Manning, 2003; Tropper and Manning, 2005, 2007). However, this problem was never encountered in the present study. Apparently, the solution properties and higher solubility combined to prevent such crystals from forming.

At the lowest KOH molality (m_{K}) of 0.0011 (Table 1), corundum solubility was determined to be $m_{\text{Al}}=0.0016 \pm 0.0004$, which is the mean of experiments KOH1 and KOH2. This is slightly greater than values reported by Becker et al. (1983) and Tropper and Manning (2007) in pure H_2O at the same conditions (0.0011 and 0.0012 molal, respectively). At the investigated P and T , m_{Al} in equilibrium with corundum increases to 2.6623 with KOH molality increasing to 3.9206 (Table 1, Fig. 2). There is no significant difference in results from the two different corundum starting materials or with the method of adding KOH. Fig. 2 shows that there is a linear increase in $\log m_{\text{Al}}$ with rising $\log m_{\text{K}}$ at high KOH concentrations ($\log m_{\text{K}} \geq -1.56$), but $\log m_{\text{Al}}$ progressively diverges from a linear dependence on $\log m_{\text{K}}$ at lower KOH concentrations.

4. Discussion

4.1. Dependence of corundum solubility on KOH concentration

A linear best fit to the data at $\log m_{\text{K}} \geq -1.56$ gives

$$\log m_{\text{Al}} = 1.004 \log m_{\text{K}} - 0.165 \quad (1)$$

($R^2 = 0.9999$). The linear slope of the change in corundum solubility with KOH at high KOH concentrations is thus ~ 1 . Working at 0.26 GPa and 700 °C, Pascal and Anderson (1989) also found a linear increase in $\log m_{\text{Al}}$ with $\log m_{\text{K}}$ with a slope of ~ 1 , although their data were collected over a much narrower range of KOH concentration (Fig. 2). At the same KOH concentration, corundum solubility is slightly higher at 0.26 GPa than at 1 GPa. This is probably due in part to the significantly smaller dissociation constant for H_2O at low P (Marshall and Franck, 1984), which yields higher pH (hence higher corundum solubility) at the same KOH concentration. The similarity between Al solubilities measured at high KOH concentrations in the two studies suggests that Al solubility at high KOH concentrations is only slightly dependent on pressure at 700 °C.

4.2. Thermodynamic implications

The increase in corundum solubility with increasing KOH concentration at 700 °C, 1 GPa, gives insight into homogeneous equilibria among aqueous species at high P and T . The solutions are expected to be slightly to strongly alkaline over the investigated range of KOH concentrations due to dissociation of the neutral KOH ion pair (KOH_{aq}) via



Accordingly, positively charged Al-hydrate species are likely negligible, and the Al-bearing species expected to predominate are neutral (e.g., $\text{HAIO}_{2,\text{aq}}$ and $\text{KAlO}_{2,\text{aq}}$) or negatively charged (e.g., AlO_2^-). (Species notation is after Johnson et al. (1992); each species is related to conventional notation through hydration reactions such as $\text{HAIO}_{2,\text{aq}} + \text{H}_2\text{O} = \text{Al}(\text{OH})_{3,\text{aq}}$ for which the standard Gibbs free energy change is zero by definition.) The implications for Al species in solution can be explored by assuming a simple set of monomeric species and the $\text{KAlO}_{2,\text{aq}}$

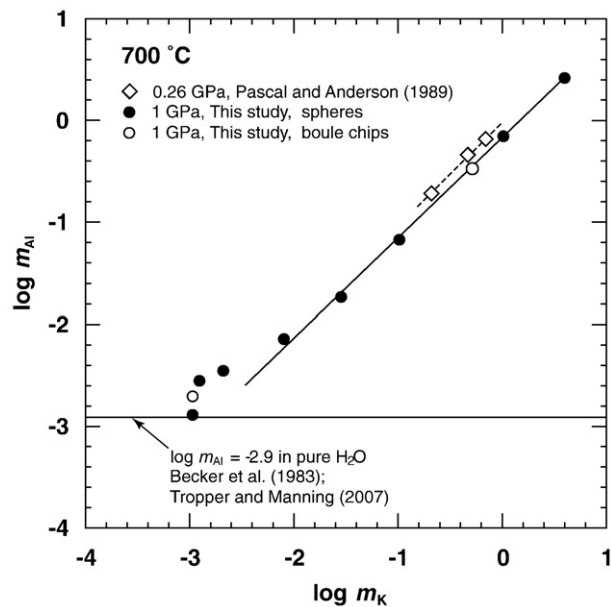


Fig. 2. Variation in corundum solubility with molality of total K (as KOH) at 700 °C and 1 GPa. Filled circles show experiments made with corundum spheres; open circles denote experiments which used corundum boule chips. Horizontal solid line shows the Al concentration determined in studies of corundum solubility in pure H_2O at these conditions (Becker et al., 1983; Tropper and Manning, 2007), illustrating that addition of KOH enhances corundum solubility relative to that in pure H_2O . The sloping solid line highlights the linear increase of Al solubility with increasing KOH at high KOH concentrations ($\log m_{\text{KOH}} = -1.56$ to 0.59). The observed slope is ~ 1 . Shown in open diamonds are the experimental results of Pascal and Anderson (1989) at 700 °C and 0.26 GPa. Their results yield the same dependence of corundum solubility on KOH concentration, although absolute solubility at a given KOH concentration is higher at 0.26 GPa.

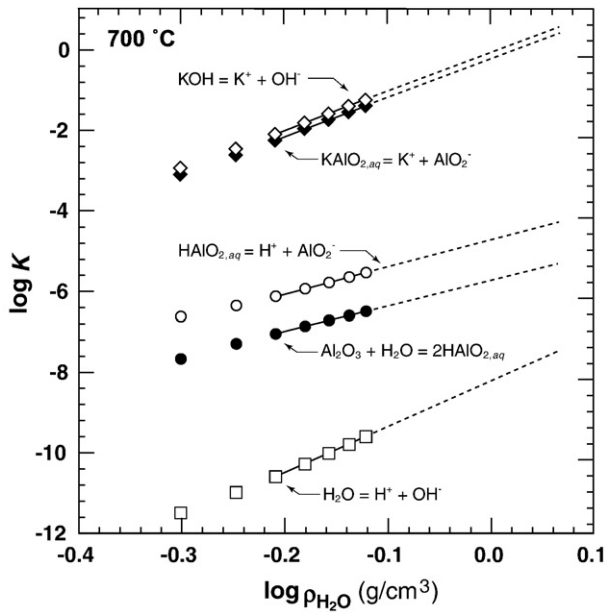


Fig. 3. Variation in $\log K$ with $\log \rho_{\text{H}_2\text{O}}$ at 700 °C for equilibria Eqs. (2)–(6). Symbols represent values calculated at 0.2–0.5 GPa, at 50 MPa increments, using SUPCRT92 with updated data from Pokrovskii and Helgeson (1995, 1997) and $\rho_{\text{H}_2\text{O}}$ from Haar et al. (1984). Above 0.3 GPa, calculated $\log K$ values are linear $\rho_{\text{H}_2\text{O}}$ within uncertainties (cf. Manning, 1998, 2007). Solid lines show linear fits to the 0.3–0.5 GPa values of $\log K$ (Eqs. (7)–(11)); dashed lines are extrapolations to 2.0 GPa.

ion pair, such that corundum solubility in KOH solutions is controlled by the combination of Eq. (2) with:



Equilibrium constants (K) for Eqs. (2)–(6) are constrained experimentally only at low pressure (if at all), and can only be calculated to ≤ 0.5 GPa using SUPCRT92 (Johnson et al., 1992). However, values at the higher P of the present study can be obtained by extrapolation using the approach of Manning (1994, 1998), which is based on the observation that the $\log K$ of homogeneous equilibria and mineral hydrolysis reactions are typically linear in $\log \rho_{\text{H}_2\text{O}}$ above 0.3 GPa. This is illustrated in Fig. 3 for Eqs. (2)–(6) at 700 °C, using thermodynamic data from Pokrovskii and Helgeson (1995, 1997; see below). It can be seen that $\log K$ values calculated from 0.2 to 0.5 GPa at 50 MPa increments exhibit linear dependence on $\log \rho_{\text{H}_2\text{O}}$ at ≥ 0.3 GPa. Linear fits at ≥ 0.3 GPa yield:

$$\log K_2 = 9.671 \log \rho_{\text{H}_2\text{O}} - 0.084 \quad (7)$$

$$\log K_3 = 6.280 \log \rho_{\text{H}_2\text{O}} - 5.732 \quad (8)$$

$$\log K_4 = 6.744 \log \rho_{\text{H}_2\text{O}} - 4.715 \quad (9)$$

$$\log K_5 = 11.356 \log \rho_{\text{H}_2\text{O}} - 8.229 \quad (10)$$

$$\log K_6 = 9.845 \log \rho_{\text{H}_2\text{O}} - 0.203 \quad (11)$$

where $\rho_{\text{H}_2\text{O}}$ is in g/cm^3 . These equations were extrapolated to H_2O density of $0.946 \text{ g}/\text{cm}^3$ at 700 °C, 1 GPa (Haar et al., 1984), to calculate $\log K$ values for Reactions 2–6 at experimental conditions (Table 2).

With the simple model expressed in Eqs. (2)–(6) for corundum solubility in KOH solutions, the results of our experiments can be used to assess the equilibrium constants for poorly constrained reactions. Manning (2007) used data derived from Pokrovskii and Helgeson (1995) to show that extrapolated $\log K$ for Reactions (3)–(5) predict corundum solubility at 700 °C, 1 GPa, in excellent agreement with measurements of Becker et al. (1983) and Tropper and Manning (2007). This indicates that values of K_3 , K_4 and K_5 (i.e., standard state thermodynamic properties of Al-hydrates and OH^-) derived from Pokrovskii and Helgeson (1995) are accurate at 700 °C and 1 GPa. Similar calculations using this approach, but with data for Al-hydrates and OH^- from other data sets (SPRONS92, Johnson et al., 1992; SLOP98, Shock et al., 1997) underpredict measured corundum solubility by more than a factor of twenty.

The accuracy of K_2 derived from Pokrovskii and Helgeson (1997) can also be assessed by comparison to experimental data. The two experimental studies which have determined K_2 at high P and T , Franck (1956) and Ho and Palmer (1997), are limited to $T \leq 600$ °C and $\rho_{\text{H}_2\text{O}} \leq 0.8 \text{ g}/\text{cm}^3$; however, in both, linear isothermal trends of $\log K_2$ with $\log \rho_{\text{H}_2\text{O}}$ provide a basis for extrapolation. Ho and Palmer (1997) gave the best-fit equation $\log K_2 = -1.183 + 132.61/T + (13.002 - 6216.8/T) \log \rho_{\text{H}_2\text{O}}$, where T is in Kelvin. This equation yields $\log K_2 = -1.206$ at 700 °C and 1 GPa (Fig. 4). A fit to the subset of the Franck (1956) data collected at high density, where linear extrapolations appear to be valid ($\rho_{\text{H}_2\text{O}} \geq 0.6 \text{ g}/\text{cm}^3$), gives

$$\log K_2 = -0.048 - 0.0011T + (6.8201 - 0.0026T) \log \rho_{\text{H}_2\text{O}} \quad (12)$$

where T is also in Kelvin (Fig. 4). Eq. (12) yields $\log K_2 = -1.222$ at 700 °C, 1 GPa. The values of $\log K_2$ predicted from the two experimental studies agree closely, but differ significantly from the value of -0.317 derived from extrapolation of the data of Pokrovskii and Helgeson (1997). Although the values of $\log K_2$ derived from all three studies are extrapolated, the trends of all isotherms (400–700 °C) with increasing density (Fig. 4) in both experimental investigations require that $\log K_2$ at 700 °C, 1 GPa, is significantly lower than -0.317 , assuming that the linear trends continue over with small density increases in dilute KOH solutions (Fig. 4).

Of all the equilibrium constants under consideration, K_6 is the most poorly constrained. No previous experiments at elevated P and T permit assessment of the accuracy of this value. Accordingly, we use the data from the present study to determine K_6 for a range of K_2 , with fixed K_3 – K_5 .

The equations necessary to constrain the activities and concentrations of the seven aqueous species expected to predominate (neglecting polymeric complexes) and appropriate equilibrium constants were derived as follows. Taking the standard states of corundum and H_2O to

Table 2
Thermodynamic data at 700 °C and 1 GPa.

System	Phase or equilibrium	Reaction	$\rho (\text{g cm}^{-3})$	$\log K$	[Source], Notes
O–H	H_2O		0.946		[1]
	$\text{H}_2\text{O} = \text{H}^+ + \text{OH}^-$	5		–8.503	[1], Eq. (10)
Al–O–H	Corundum + $\text{H}_2\text{O} = 2\text{HAIO}_{2,\text{aq}}$	3		–5.883	[2], Eq. (8)
	$\text{HAIO}_{2,\text{aq}} + \text{H}^+ + \text{AlO}_2^-$	4		–4.877	[2], Eq. (9)
K–Al–O–H	$\text{KOH} = \text{K}^+ + \text{OH}^-$	2		–0.317	[3], Eq. (7)
	$\text{KOH} = \text{K}^+ + \text{OH}^-$	2		–1.222	[4], Eq. (12)
	$\text{KOH} = \text{K}^+ + \text{OH}^-$	2		–1.206	[5]
	$\text{KAlO}_2 = \text{K}^+ + \text{AlO}_2^-$	6		–0.440	[3], Eq. (11)
	$\text{KAlO}_2 = \text{K}^+ + \text{AlO}_2^-$	6		–0.349	[6], using K_2 from [4]
	$\text{KAlO}_2 = \text{K}^+ + \text{AlO}_2^-$	6		–0.299	[6], using K_2 from [5]

Sources: [1] SUPCRT92 (Johnson et al., 1992); [2] Pokrovskii and Helgeson (1995); [3] Pokrovskii and Helgeson (1997); [4] Franck (1956); [5] Ho and Palmer (1997); [6] this study. Values given for Reactions 3 and 4 differ slightly from Manning (2007) due to the use of different H_2O properties in this study.

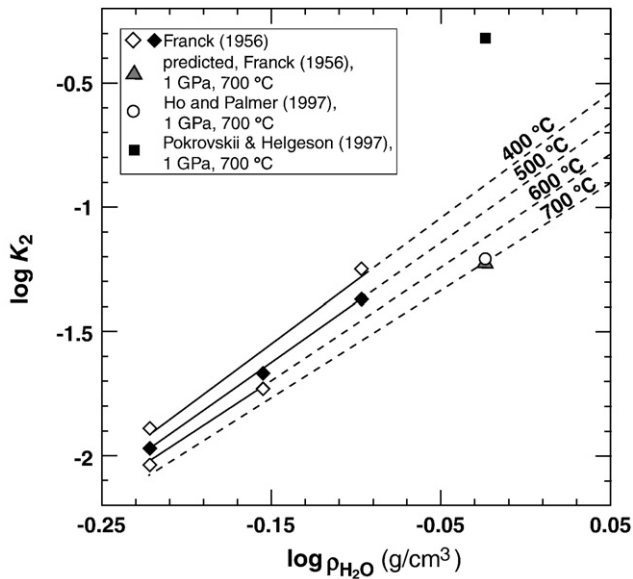


Fig. 4. Logarithmic plot of $\rho_{\text{H}_2\text{O}}$ versus the equilibrium constant for KOH_{aq} dissociation (K_2). Diamonds show values of Franck (1956), based on electrical conductance measurements between 400 to 600 °C. Only data from $\rho_{\text{H}_2\text{O}} \geq 0.6 \text{ g/cm}^3$ are shown. Solid lines show the fit to the high- P data (Eq. (12)); dashed lines show isothermal extrapolation to higher T and H_2O density. The predicted value of $\log K_2$ at 700 °C, 1 GPa, is highlighted with a shaded triangle. The open circle shows the values of $\log K_2$ calculated from Ho and Palmer (1997), and the filled square represents the value based on Pokrovskii and Helgeson (1997) (Eq. (7)).

be unit activity of the pure phase at any P and T , four constraints are provided by the mass-action expressions for Eqs. (2)–(5)

$$K_2 = \frac{a_{\text{K}^+} + a_{\text{OH}^-}}{a_{\text{KOH}_{\text{aq}}}} \quad (13)$$

$$K_3 = a_{\text{HAIO}_{2,\text{aq}}}^2 \quad (14)$$

$$K_4 = \frac{a_{\text{H}^+} + a_{\text{AlO}_2^-}}{a_{\text{HAIO}_{2,\text{aq}}}} \quad (15)$$

$$K_5 = a_{\text{H}^+} + a_{\text{OH}^-} \quad (16)$$

where a is activity of the subscripted species. Three additional constraints are provided by Al and K mass balance and charge balance:

$$m_{\text{K}} = m_{\text{K}^+} + m_{\text{KOH}_{\text{aq}}} + m_{\text{KAlO}_{2,\text{aq}}} \quad (17)$$

$$m_{\text{Al}} = m_{\text{HAIO}_{2,\text{aq}}} + m_{\text{AlO}_2^-} + m_{\text{KAlO}_{2,\text{aq}}} \quad (18)$$

$$m_{\text{H}^+} + m_{\text{K}^+} = m_{\text{OH}^-} + m_{\text{AlO}_2^-} \quad (19)$$

Adopting a standard state for solutes of unit activity in the hypothetical 1 molal solution referenced to infinite dilution, and assuming unit activity coefficient for neutral species, the concentrations of species can be substituted for activities in Eqs. (13)–(15) using $a_i = \gamma_i m_i$, where γ_i is activity coefficient of the subscripted species, which can be computed from a suitable activity model for ions. These calculations employed the Güntelberg equation,

$$\log \gamma_i = - \frac{Az_i^2 \sqrt{I}}{1 + \sqrt{I}} \quad (20)$$

where z is ion charge, I is ionic strength, and A is the solvent parameter, here assumed to be unity following arguments of Manning (1998, 2007). The Güntelberg equation was used because of its simplicity and the absence of constraints on activity coefficients at the

P and T of this study (trial calculations using the Davis (1962) equation gave nearly identical results). The resulting set of equations can be solved for the concentrations and activities to obtain a_{K^+} , $a_{\text{AlO}_2^-}$, and $a_{\text{KAlO}_{2,\text{aq}}}$ and hence K_6 via

$$K_6 = \frac{a_{\text{K}^+} + a_{\text{AlO}_2^-}}{a_{\text{KAlO}_{2,\text{aq}}}} \quad (21)$$

for each experiment. In principle, a simple weighted mean of K_6 values would be obtained by this approach. However, due to the scatter of the experimental data, several results yielded negative concentrations of some species, and therefore meaningless K_6 values. For this reason we utilized an alternative solution strategy, in which a trial value of K_6 was refined by minimizing χ^2 for calculated vs. observed m_{K} using the full set of experiments.

Use of the experimentally based K_2 from Ho and Palmer (1997) yields $\log K_6 = -0.299$ ($\chi^2 = 0.36$) and excellent match with the experimental data (Fig. 5). Nearly identical results were obtained from K_2 derived from Franck (1956): $\log K_6 = -0.349$ ($\chi^2 = 0.36$). These values of $\log K_6$ based on experimentally constrained K_2 are close to $\log K_6$ derived from Pokrovskii and Helgeson (1997) (-0.440 ; Table 2). In contrast, using K_2 derived from Pokrovskii and Helgeson (1997) leads to $\log K_6 = 6.080$, with higher χ^2 of 1.16 and systematic underprediction of m_{K} at experimental $m_{\text{K}} \geq 0.0079$. Thus, the values of K_2 and K_6 derived from Pokrovskii and Helgeson (1997) are mutually inconsistent. Pokrovskii and Helgeson (1997) compared their $\log K_2$ with Franck's (1956) experiments over a range of P and T in their Fig. 2, where it is evident that the values they calculated are systematically higher than experimental data at high H_2O density, and that the discrepancy grows larger with increasing P . The combination of low χ^2 and good agreement with the independently derived value for K_6 therefore support use of K_2 from Franck (1956) or Ho and Palmer (1997) with K_6 constrained by the present experimental results (Table 2). Because Ho and Palmer (1997) made more measurements which better constrain extrapolations, it is recommended that the K_2 derived from their study be used at high P and T .

It is important to note that it is possible in principle to simultaneously refine K_2 and K_6 using our approach. A minimum χ^2 of 0.355 was obtained for $\log K_2 = -2.241$ and $\log K_6 = -1.868$; however, this value of K_2 is nearly 10 times lower than that predicted

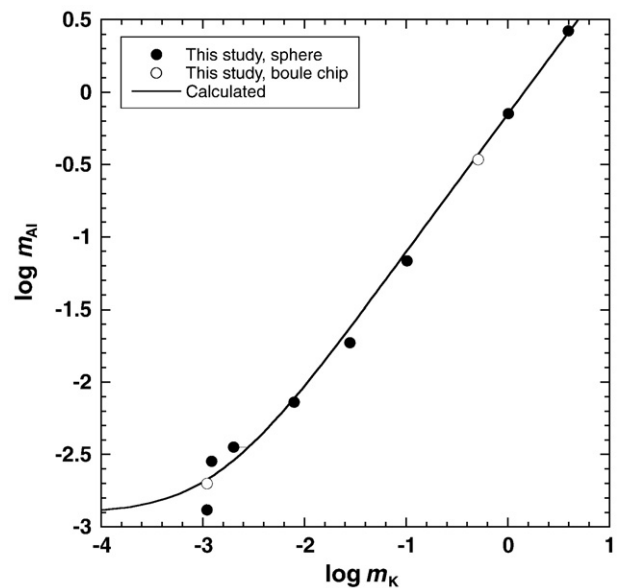


Fig. 5. Logarithmic plot of total K molality vs. total Al molality at 700 °C and 1 GPa. The plot highlights the agreement between experimentally determined total Al (circles) with that calculated (solid curve) using preferred equilibrium constants (Table 2).

by extrapolation of the Franck (1956) and Ho and Palmer (1997) results, whereas the extrapolation should yield a minimum value given the possible, very slight curvature evident in some of the experimental data (Fig. 4). Significantly, there is a broad minimum in χ^2 vs. K_2 , which indicates that the data lack the precision to provide a robust simultaneous constraint on both equilibrium constants. We conclude that the most accurate constraint afforded by our experimental data is the refined value of $K_6 = 0.502$ at 700 °C and 1 GPa.

The model for corundum solubility successfully accounts for the dependence of corundum solubility on KOH concentration and is likely adequate given the paucity of experimental constraints; however, as more data become available, it should be possible to assess several of the assumptions. First, the activity model for ions is necessarily simplistic. Calculated values of activity coefficients of monovalent ions ranged from 0.93 at $m_K = 0.001$ to 0.25 at $m_K = 3.921$. These values will change with an alternate formulation and different values of the solvent parameter A , though such changes will not significantly affect the conclusions of the present study. In addition, unit activity coefficients were adopted for neutral species. This assumption could break down at high concentrations or in the presence of significant polymerization. Nevertheless, despite these caveats, it is clear that the simple model for corundum solubility is sufficient to explain the experimental data.

4.3. Predicted concentrations of aqueous species at 700 °C, 1 GPa

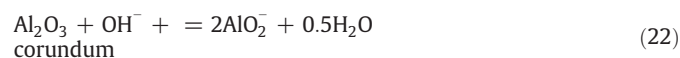
The abundance of the most important aqueous species at 700 °C and 1 GPa in corundum-saturated KOH-bearing solutions can be calculated in light of the equilibrium constants derived above and using the same activity-coefficient model and assumptions (Fig. 6). Fig. 6A shows aqueous species abundance in equilibrium with corundum at 700 °C, 1 GPa, in the system Al–K–O–H. As total KOH concentration increases, there is a rise in OH^- due to the predominance of K^+ . This yields a commensurate increase in dissolved Al as Eq. (4) is driven to the right, producing AlO_2^- from $\text{HAIO}_{2,\text{aq}}$ and hence higher corundum solubility (Eq. (3)). The predicted mole-for-mole increase in Al with K at $m_K > 0.01$ is consistent with our experimental findings (Fig. 2). The $\text{KAIO}_{2,\text{aq}}$ ion pair increases with m_K , as required by the law of mass action; however, in this simple system, it is always the least abundant K-bearing species, and is never the predominant Al species over the plotted range.

For the purposes of comparison of Al solubility in the K–Al–O–H system to that in other systems, it is useful to use pH as the independent variable instead of total K concentration (Fig. 6B). The preferred equilibrium constants (Table 2) yield a calculated pH range for our experiments of 4.7–7.5. The dominant species in the three experiments with the lowest K contents (<0.002 molal; Table 1) is predicted to be $\text{HAIO}_{2,\text{aq}}$; however, at higher m_K , AlO_2^- should predominate. $\text{KAIO}_{2,\text{aq}}$ is predicted to become the dominant Al species only at extremely high pH of >8 (Fig. 6B). Fig. 6B allows comparison of our results with experimental studies on corundum solubility in H_2O at the same P and T (Becker et al., 1983; Tropper and Manning, 2007). Again, the thermodynamic data yield excellent agreement between predicted and observed total Al concentrations. The expected lower pH is calculated to be 3.9. This is slightly lower than acid–base neutrality at these conditions (4.2) due to the presence of AlO_2^- as a subordinate constituent, which requires higher activity of charge-balancing H^+ relative to pure H_2O .

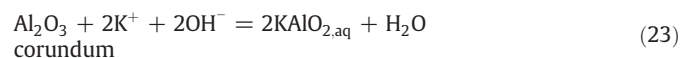
4.4. Implications for high-PT fluids

Our results offer new constraints on the thermodynamics of KOH_{aq} dissociation and the occurrence of the $\text{KAIO}_{2,\text{aq}}$ ion pair in high-PT geologic fluids. The dissociation of KOH_{aq} strongly influences Al solubility in high-PT fluids, due to the possibility that either AlO_2^- or $\text{KAIO}_{2,\text{aq}}$ is abundant in KOH-rich solutions. If Eq. (2) is driven to the

right, higher solubility of corundum will result due to the progress of the reactions



and



Our conclusion that K_2 is best approximated at 700 °C, 1 GPa, by the value derived from Ho and Palmer (1997) implies that KOH_{aq} is less dissociated in high-PT fluids than would have been inferred from the results of Pokrovskii and Helgeson (1997). For example, the pH of a 0.1 molal KOH solution at 700 °C, 1 GPa, is predicted to be 70%

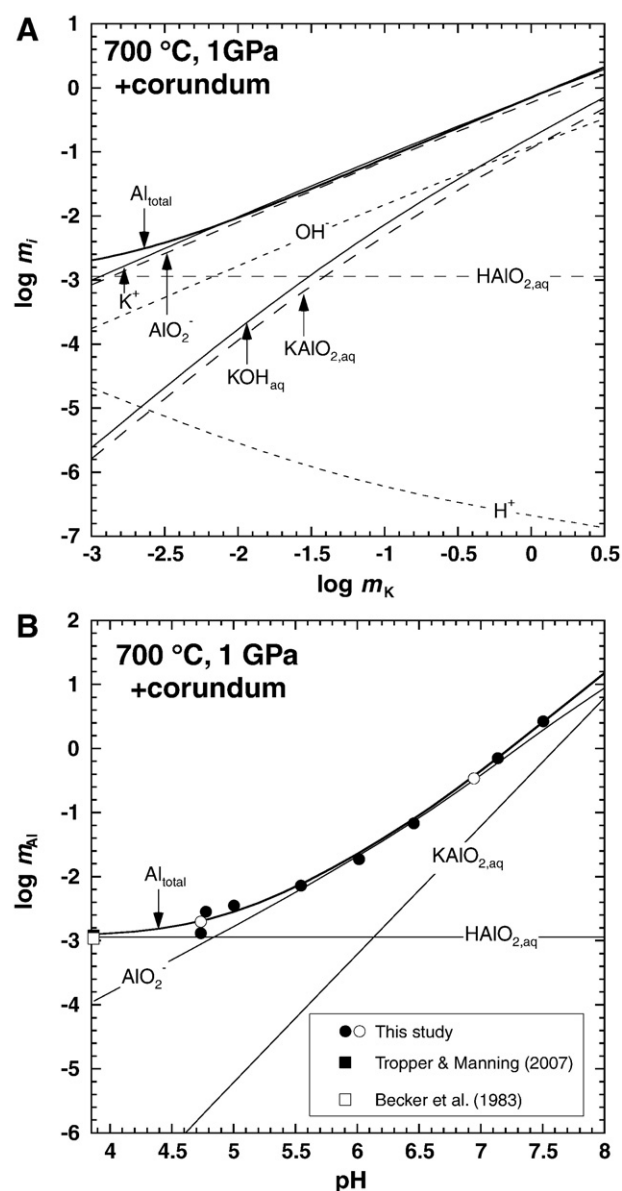


Fig. 6. (A) Equilibrium abundance of aqueous species at corundum saturation as a function of total K molality in the system Al–K–O–H at 700 °C and 1 GPa. (B) Variation in corundum solubility with pH in aqueous KOH solution at 700 °C and 1 GPa. Solid lines show predicted total m_{Al} and abundances of Al-bearing aqueous species. Circles show data from this study (filled, spheres; open, boule chips); squares show corundum solubility in pure H_2O (Becker et al., 1983; Tropper and Manning, 2007).

dissociated using our recommended K_2 , whereas it would be 94% dissociated if the Pokrovskii and Helgeson (1997) results were used. This translates to a slightly lower pH (7.1 vs. 7.2); that is, KOH is a slightly weaker base using our preferred value of K_2 .

Our result also indicates that the $\text{KAlO}_{2,\text{aq}}$ ion pair is of only minor importance in high- PT fluids lacking significant additional potassium salts (e.g., KCl, KF, or K_2CO_3). Thus, Eq. (22) accounts for substantially more dissolved Al than Eq. (23) at the conditions investigated. Fig. 6 illustrates that $\text{KAlO}_{2,\text{aq}}$ will not be the predominant reservoir for Al except at extremely high pH values. In rocks interacting with initially pure H_2O , hydrolysis reactions tend to produce alkaline pH; however, at high P and T , the large dissociation constant for H_2O inhibits extremes in pH (Manning, 2004). When coupled with the tendency of any free chloride, sulfate, or other acid-forming anions to keep pH low, it can be concluded that conditions which would favor predominance of $\text{KAlO}_{2,\text{aq}}$ over other Al-bearing aqueous species are likely quite rare in the Earth's crust and upper mantle.

5. Conclusions

- (1) The addition of KOH to H_2O at 700 °C and 1 GPa significantly enhances the solubility of corundum relative to that in pure H_2O .
- (2) The experimental results constrain the equilibrium constant for $\text{KAlO}_{2,\text{aq}}$ dissociation (K_6) to be 0.502 at 700 °C, 1 GPa, using K_2 derived from the Ho and Palmer (1997) data, in good agreement with the value for K_6 extrapolated from data of Pokrovskii and Helgeson (1997). However, when K_2 was derived from Pokrovskii and Helgeson (1997), an unreasonably high value of 1.2×10^6 was obtained, with poor goodness-of-fit statistics. We therefore recommend use of K_2 from Ho and Palmer (1997) along with our new value of K_6 at the conditions of investigated in this study.
- (3) Thermodynamic data constrained by the new experimental results permit calculation of heterogeneous equilibria in the system K-Al-O-H at 700 °C and 1 GPa. At low total K concentrations the dominant Al species in solution is the neutral Al hydrate $\text{HAlO}_{2,\text{aq}}$. As m_{K} increases, pH and AlO_2^- rise, causing an increase in m_{Al} . The $\text{KAlO}_{2,\text{aq}}$ ion pair becomes more abundant than $\text{HAlO}_{2,\text{aq}}$ at pH = 6.2, but is never predicted to be the predominant Al-bearing species at the conditions examined experimentally. Because pH values in excess of those of the present experiments are probably rare in natural high P - T systems, Al transport as $\text{KAlO}_{2,\text{aq}}$ is unlikely in chloride-free geologic fluids.

Acknowledgments

This study was supported by Swiss National Science Foundation grant PBLA2-109963 and U.S. National Science Foundation grants EAR-0337170 and EAR-0711521 to CEM. We thank Robert Newton for advice and assistance in the piston-cylinder laboratory, and John Walther and an anonymous reviewer for insightful comments that improved the manuscript.

References

- Ague, J.J., 1995. Deep-crustal growth of quartz, kyanite and garnet into large-aperture, fluid-filled fractures, north-eastern Connecticut, USA. *Journal of Metamorphic Geology* 13, 299–314.
- Akerlof, G., Bender, P., 1941. The density of aqueous solutions of potassium hydroxide. *Journal of the American Chemical Society* 63, 1085–1088.
- Anderson, G.M., 1995. Is there alkali-aluminum complexing at high temperatures and pressures? *Geochimica et Cosmochimica Acta* 59, 2155–2161.
- Anderson, G.M., Burnham, C.W., 1967. Reaction of quartz and corundum with aqueous chloride and hydroxide solutions at high temperature and pressure. *American Journal of Science* 265, 12–27.
- Anderson, G.M., Burnham, C.W., 1983. Feldspar solubility and the transport of aluminum under metamorphic conditions. *American Journal of Science* 283, 283–297.
- Antignano, A., Manning, C.E., 2008a. Apatite solubility in H_2O and $\text{H}_2\text{O-NaCl}$ at 700 to 900 °C and 0.7 to 2.0 GPa. *Chemical Geology* 251, 112–119.
- Antignano, A., Manning, C.E., 2008b. Rutile solubility in H_2O , $\text{H}_2\text{O-SiO}_2$ and $\text{H}_2\text{O-NaAlSi}_3\text{O}_8$ at 0.7–2.0 GPa and 700–1000 °C: implications for mobility of nominally insoluble elements in geologic fluids. *Chemical Geology* 255, 283–293.
- Azaroual, M., Pascal, M.L., Roux, J., 1996. Corundum solubility and aluminum speciation in KOH aqueous solutions at 400 °C from 0.5 to 2.0 kbar. *Geochimica et Cosmochimica Acta* 60, 4601–4614.
- Barns, R.L., Laudis, R.A., Shield, R.M., 1963. The solubility of corundum in basic hydrothermal solvents. *Journal of Physical Chemistry* 67, 835–839.
- Becker, K.H., Cemic, L., Langer, K.E.O.E., 1983. Solubility of corundum in supercritical water. *Geochimica et Cosmochimica Acta* 47, 1573–1578.
- Beitter, T., Wagner, G., Markl, G., 2008. Formation of kyanite-quartz veins of the Alpe Sponda, Central Alps, Switzerland: implications for Al transport during regional metamorphism. *Contributions to Mineralogy and Petrology* 156, 689–707.
- Caciagli, N.C., Manning, C.E., 2003. The solubility of calcite in water at 5–16 kbar and 500–800 °C. *Contributions to Mineralogy and Petrology* 146, 275–285.
- Carmichael, D.M., 1969. On the mechanism of prograde metamorphic reactions in quartz-bearing pelitic rocks. *Contribution to Mineralogy and Petrology* 20, 244–267.
- Castet, S., Dandurand, J.L., Schott, J., Gout, R., 1992. Experimental study of aluminium hydrolysis and complexation with acetate and sodium ions in hydrothermal solutions. In: Kharaka, Y.K., Maest, A.S. (Eds.), *Water Rock Interaction*. Balkema, 1013–1016.
- Davis, C.W., 1962. *Ion Association*. Butterworths, London, 189 pp.
- Diakonov, I., Pokrovskii, G., Schott, J., Castet, S., Gout, R., 1996. An experimental and computational study of sodium-aluminum complexing in crust fluids. *Geochimica et Cosmochimica Acta* 60, 197–211.
- Franck, E.U., 1956. Hochverdichteter Wasserdampf III. Ionendissoziation von HCl, KOH and H_2O in ueberkritischem Wasser. *Zeitschrift fuer Physikalische Chemie, Neue Folge*, vol. 8, 192–206.
- Haar, L., Gallagher, J.S., Kell, G.S., 1984. NBS/NRC Steam Tables. Hemisphere, New York, p. 320.
- Hemley, J.J., Jones, W.R., 1964. Chemical aspects of hydrothermal alteration with emphasis on hydrogen metasomatism. *Economic Geology* 59, 538–569.
- Ho, P.C., Palmer, D.A., 1997. Ion association of a dilute aqueous potassium chloride and potassium hydroxide solutions to 600 °C and 300 MPa determined by electrical conductance measurements. *Geochimica et Cosmochimica Acta* 61, 3027–3040.
- Johnson, J.W., Oelkers, E.H., Helgeson, H.C., 1992. SUPCRT92: a software package for calculating the standard molal thermodynamic properties of minerals, gases, aqueous species, and reactions from 1 to 5000 bars and 0 to 1000 °C. *Computers & Geosciences* 18, 899–947.
- Kerrick, D.M., 1988. Al_2SiO_5 -bearing segregations in the Lepontine Alps, Switzerland: aluminum mobility in metapelites. *Geology* 16, 636–640.
- Manning, C.E., 1994. The solubility of quartz in H_2O in the lower crust and upper mantle. *Geochimica et Cosmochimica Acta* 58, 4831–4839.
- Manning, C.E., 1998. Fluid composition at the blueschist-eclogite transition in the model system $\text{Na}_2\text{O-Al}_2\text{O}_3\text{-SiO}_2\text{-H}_2\text{O-HCl}$. *Schweizerische Mineralogische Und Petrographische Mitteilungen* 78, 225–242.
- Manning, C.E., 2004. The chemistry of subduction-zone fluids. *Earth and Planetary Science Letters* 223, 1–16.
- Manning, C.E., 2007. Solubility of corundum + kyanite in H_2O at 700 °C and 10 kbar: evidence for Al-Si complexing at high pressure and temperature. *Geofluids* 7, 258–269.
- Manning, C.E., Boettcher, S.L., 1994. Rapid-quench hydrothermal experiments at mantle pressures and temperatures. *American Mineralogist* 79, 1153–1158.
- Marshall, W.L., Franck, E.U., 1984. Ion product of water substance, 0–1000 °C, 1–10,000 bars: new international formulation and its background. *Journal of Physical and Chemical Reference Data* 10, 295–304.
- McLelland, J., Morrison, J., Selleck, B., Cunningham, B., Olsen, C., Schmidt, K., 2002. Hydrothermal alteration of late- to post-tectonic Lyon Mountain Granitic Gneiss, Adirondack Mountains, New York. Origin of quartz-sillimanite segregations, quartz-albite lithologies, and associated Kiruna-type low-Ti Fe-oxide deposits. *Journal of Metamorphic Geology* 20, 175–190.
- Nabelek, P.L., 1997. Quartz-sillimanite leucosomes in high-grade schists, Black Hills, South Dakota: a perspective on the mobility of Al in high-grade metamorphic rocks. *Geology* 25, 995–998.
- Newton, R.C., Manning, C.E., 2006. Solubilities of corundum, wollastonite and quartz in $\text{H}_2\text{O-NaCl}$ solutions at 800 °C and 10 kbar: interaction of simple minerals with brines at high pressure and temperature. *Geochimica et Cosmochimica Acta* 70, 5571–5582.
- Newton, R.C., Manning, C.E., 2007. Solubility and stability of grossular, $\text{Ca}_3\text{Al}_2\text{Si}_3\text{O}_{12}$, in the system $\text{CaSiO}_3\text{-Al}_2\text{O}_3\text{-NaCl-H}_2\text{O}$ at 800 °C and 10 kbar. *Geochimica et Cosmochimica Acta* 71, 5191–5202.
- Newton, R.C., Manning, C.E., 2008. Solubility of corundum in the system $\text{Al}_2\text{O}_3\text{-SiO}_2\text{-H}_2\text{O-NaCl}$ solutions at 800 °C and 10 kbar. *Chemical Geology* 249, 250–261.
- Pascal, M.L., Anderson, G.M., 1989. Speciation of Al, Si and K in supercritical solutions: experimental study and interpretation. *Geochimica et Cosmochimica Acta* 55, 1843–1855.
- Pokrovskii, V.A., Helgeson, H.C., 1995. Thermodynamic properties of aqueous species and the solubilities of minerals at high pressures and temperatures: the system $\text{Al}_2\text{O}_3\text{-H}_2\text{O-NaCl}$. *American Journal of Science* 295, 1255–1342.
- Pokrovskii, V.A., Helgeson, H.C., 1997. Thermodynamic properties of aqueous species and solubilities of minerals at high pressure and temperatures: the system $\text{Al}_2\text{O}_3\text{-H}_2\text{O-KOH}$. *Chemical Geology* 137, 221–242.
- Ragnasdottir, K., Walther, J., 1985. Experimental determination of corundum solubilities in pure water between 400–700 °C and 1–3 kbar. *Geochimica et Cosmochimica Acta* 49, 2109–2115.
- Shock, E.L., Sassani, D.C., Willis, M., Sverjensky, D.A., 1997. Inorganic species in geologic fluids: correlations among standard molal thermodynamic properties of aqueous ions and hydroxide complexes. *Geochimica et Cosmochimica Acta* 61, 907–950.

- Tropper, P., Manning, C.E., 2005. Very low solubility of rutile in H₂O at high pressure and temperature, and its implications for Ti mobility in subduction zones. *American Mineralogist* 90, 502–505.
- Tropper, P., Manning, C.E., 2007. The solubility of corundum in H₂O at high pressure and temperature and its implication for Al mobility in the deep crust and upper mantle. *Chemical Geology* 240, 54–60.
- Walther, J.V., 1997. Experimental determination and interpretation of the solubility of corundum in H₂O between 350 and 600 °C from 0.5 to 2.2 kbar. *Geochimica et Cosmochimica Acta* 61, 4955–4964.
- Walther, J.V., Woodland, A.B., 1993. Experimental determination and interpretation of the solubility of the assemblage microcline, muscovite and quartz in supercritical H₂O. *Geochimica et Cosmochimica Acta* 57, 2431–2437.
- Widmer, T., Thompson, A.B., 2001. Local origin of high pressure vein material in eclogite facies rocks of the Zermatt–Saas Zone, Switzerland. *American Journal of Sciences* 301, 627–656.
- Woodland, A.B., Walther, J.V., 1987. Experimental determination of the solubility of the assemblage paragonite, albite, and quartz in supercritical H₂O. *Geochimica et Cosmochimica Acta* 51, 365–372.
- Yardley, B.W.D., 1977. The nature and significance of the mechanism of sillimanite growth in the Connemara Schist, Ireland. *Contribution to Mineralogy and Petrology* 65, 53–58.